Available online at www.sciencedirect.com
SCIENCE DIRECT®
Journal of Power Sources 124 (2003) 65–75
JOURNAL OF POWER SOURCES
www.elsevier.com/locate/jpowsour

Combinations of solid oxide fuel cell and several enhanced gas turbine cycles

Prapan Kuchonthara [a], Sankar Bhattacharya [b], Atsushi Tsutsumi [a,*]

[a] *Department of Chemical System Engineering, The University of Tokyo, 7-3-1 Hongo, Bunkyo-ku, Tokyo 113-8656, Japan*
[b] *Cooperative Research Centre for Clean Power from Lignite, 8/677 Springvale Road, Mulgrave 3170, Vic., Australia*

Received 7 April 2003; received in revised form 5 June 2003; accepted 11 June 2003

Abstract

Combined power generation systems with combinations of solid oxide fuel cell (SOFC) and various enhanced gas turbine (GT) cycles were evaluated. In the GT part, steam injected gas turbine (STIG) cycle, GT/steam turbine (ST) combined cycle, and humid air turbine (HAT) cycle were considered. Moreover, additional recuperation was considered by means of air preheating (APH) in the STIG cycle. Effects of operating turbine inlet temperature (TIT) and pressure ratio (PR) on overall system performance were assessed. Although the SOFC–HAT system shows the lowest specific work output compared to other systems, its highest thermal efficiency presents a significant advantage. Furthermore, at high TITs and PRs the SOFC–HAT system gives the best performance in terms of both thermal efficiency and specific work. Results indicate that energy recuperative features in the HAT promote the positive effect of increasing TIT by means of enhancing GT efficiency, leading to the improvement in thermal efficiency of the overall system.

Keywords: Solid oxide fuel cell; Gas turbine; HAT cycle; Combined cycle; Power generation system

1. Introduction

Among the different fuel cells under development today, the solid oxide fuel cell (SOFC) is particularly interesting because of its high operating temperature (ca. 1273 K). This high temperature allows use of non-noble catalysts, which are less expensive and insensitive to certain fuel contaminants. Furthermore, their use contributes to suitability of integration with gas turbine (GT) cycles. In this scheme, heat generated by electrochemical reactions in SOFC is utilized for more power generation in GT by means of elevated pressure operations. This enables improved overall efficiency with respect to an individual system. However, the power ratio of SOFC to GT is high because SOFC is more efficient than GT in terms of energy conversion. This makes the combined system costly. Therefore, an improvement of GT efficiency is essential from this point of view.

Waste heat recovery from turbine exhaust is known to improve GT performance significantly. In general, employing steam turbine (ST) cycles can provide the best performance. Heat of GT exhaust is recovered in a heat recovery steam generator (HRSG) to generate steam for the bottoming ST cycle. This scheme is widely called a combined cycle power generation system. However, such a system requires a large bundle of equipment for ST cycles and seems to be complicated and costly. The steam injection cycle is thus the first approach that was developed, it is generally known as a steam injected gas turbine (STIG) cycle. Exhaust gases are employed to create steam that is expanded in the GT itself. In contrast to the combined cycle, the STIG cycle can enhance system performance without the ST cycle [1–4].

In addition, an advanced recuperative GT cycle has been proposed: the humid air turbine (HAT) cycle [5]. In this cycle, hot water is evaporated into compressed air in a humidifier (HF) unit. Even though this configuration requires no ST cycle, the combination of processes of water-vapor addition (humidification) and compressor intercooling enhances both power and efficiency. High performance with minimal construction area is a HAT cycle merit, making the cycle competitive with the combined cycle [6–8].

Although several combinations of SOFC and GT cycles have been proposed, only heat recuperation has been incorporated in SOFC–GT combined systems by means of air preheating (APH) [9–13]. Our previous work exhibited the positive effect of energy recovery from GT exhaust in the SOFC–GT cycle by means of heat and steam recuperation [14]. Results indicated that enrichment of GT performance

* Corresponding author. Tel.: +81-3-5841-7336; fax: +81-3-5841-7270.
E-mail address: tsutsumi@chemsys.t.u-tokyo.ac.jp (A. Tsutsumi).

0378-7753/$ – see front matter © 2003 Elsevier B.V. All rights reserved.
doi:10.1016/S0378-7753(03)00740-7

Nomenclature

LHV	lower heating value of fuel ($J\,kg^{-1}$)
m	mass flow rate ($kg\,s^{-1}$)
w	specific work ($J\,kg^{-1}$)
W	work ($J\,s^{-1}$)

Greek letter

η_{th}	thermal efficiency, LHV basis (–)

Subscripts

air	air
CP	compressor
f	fuel
FC	fuel cell
GT	gas turbine
ST	steam turbine

contributes to an improvement of overall system efficiency. So far, few studies have been conducted on the combination with enhanced GT cycles such as the STIG cycle, GT/ST combined cycle, and the HAT cycle. This study examines SOFC–GT combined systems with STIG, GT/ST, and HAT cycles using a process simulation tool, ASPEN Plus.

2. Combined system configuration and methodology

The SOFC model employed in this study was explained in our previous work [14]. Model calculations were performed by Fortran calculations in ASPEN Plus, whereas other components constituting the system were modeled as standard unit operation models. Schematic diagrams of the SOFC–GT/ST, SOFC–STIG, and SOFC–HAT are illustrated in Figs. 1–3, respectively.

The SOFC–GT/ST employs the ST cycle as a bottoming cycle. The GT exhaust is used to generate steam in a HRSG. This steam is supplied to the ST cycle for further power generation. In this work, the ST cycle mainly comprises heat exchangers and ST with three pressure levels: high-pressure (HP), intermediate pressure (IP), and low-pressure (LP) [15].

In SOFC–STIG systems, the steam generated in a HRSG using GT exhaust is directly injected to the combustion chamber (CC) and simultaneously expanded in the GT together with combustion gases and air streams. In general, steam pressure in this cycle is slightly higher by 2–3% than the pressure level in the CC for the purpose of steam injection. The generated steam temperature is determined by the minimum temperature approach in the HRSG.

In addition to the simple SOFC–STIG, an APH feature was considered for incorporation into the system. In this case, GT exhaust is used not only to generate injected steam by the HRSG, but also to preheat compressed air stream using a recuperator. The preheated air temperature is determined by recuperator efficiency. A schematic diagram

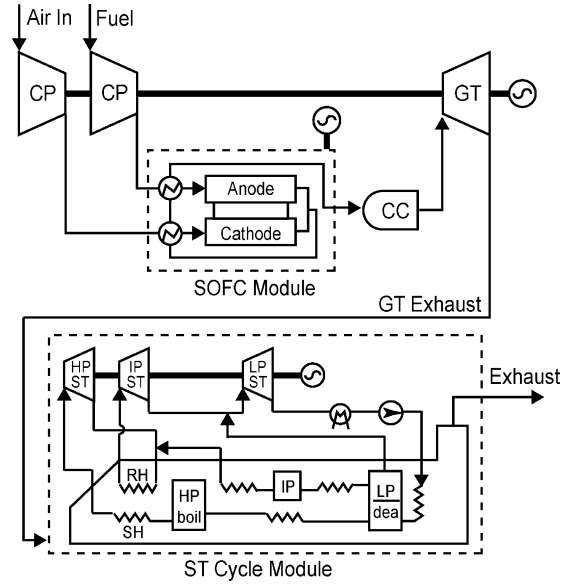

Fig. 1. Schematic of a SOFC–GT/ST system.

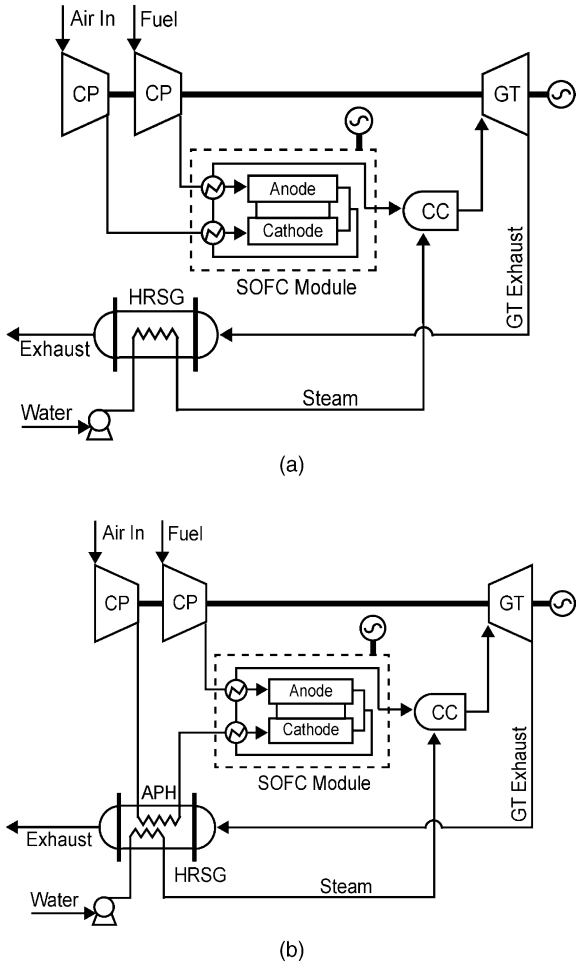

Fig. 2. Schematic of a SOFC–STIG system: (a) simple system; (b) system with APH.

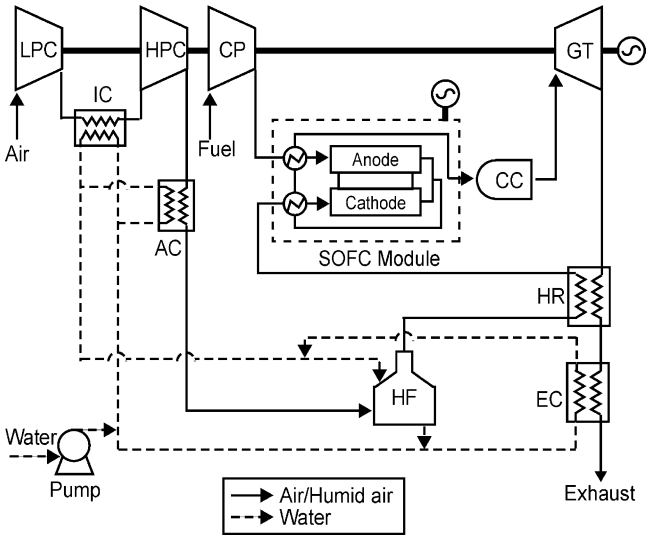

Fig. 3. Schematic of a SOFC–HAT system.

of the SOFC–STIG with such an APH system is illustrated in Fig. 2(b).

The SOFC–HAT system mainly consists of low-pressure and high-pressure air compressors (LPC and HPC), an intercooler (IC), an aftercooler (AC), a HF, mixers, pumps, a SOFC unit with heat exchanger system, a CC, a GT, a heat recovery (HR) unit, and an economizer (EC). Heat of the GT exhaust is recovered in the HR unit to preheat humid air generated by the HF prior to its admission in the SOFC part and the CC. Temperature of the humid air was determined by the minimum temperature approach in the HR unit. Heat of the low temperature exhaust is completely recovered in the EC to heat circulating water from the HF. Hot water streams after IC and AC are mixed together with circulating water from the EC. Mixed hot water is fed to the HF, where it is evaporated into depleted compressed air, generating humid air. During simulation, we confirmed that temperature of the hot water stream prior to evaporation did not exceed saturation temperature. Make-up water is supplied to compensate for the amount of water evaporated in the HF.

The systems mentioned above were simulated and evaluated with the following hypotheses: (a) hydrogen (H_2) was used as fuel; (b) working pressure ratios (PRs) of 5, 7, 10, and 15 were considered; (c) thermodynamic properties based on the Peng–Robinson equation of state with the Boston–Mathias alpha function, which is appropriate for power generation process, were used; (d) thermodynamic properties of gases, liquid water, and steam were taken from databases available in the ASPEN Plus; (e) isentropic efficiency of 0.9 for both compression and expansion processes was given; (f) equivalent PRs were given for the LPC and HPC in the case of SOFC–HAT system; (g) no additional turbine blade cooling was considered; (h) a pressure loss of 2–3% was allotted to heat exchangers, SOFC stacks, the HRSG, and the GT CC; (i) the minimum temperature approach in the HR unit was 20 K; (j) recuperator efficiency of 0.8 was considered; (k) current density and cell operating temperature in the SOFC were set as certain values for all system analyses; (l) final temperature of exhaust gas from the HRSG or the EC (in case of the SOFC–HAT) was 423 K, which was higher than the corresponding dew point temperature to prevent condensation problems. Table 1 summarizes the basic assumptions and input parameters of the system simulation.

Table 1
Assumptions and configurations for system evaluation

SOFC	
DC–AC converter efficiency	0.95
Fuel utilization factor, U_f	0.45–0.95
Air utilization factor, U_a	0.30
Cell operating temperature	1273 K
Area-specific resistance	0.5 Ω cm^2
Current density	400 mA/cm^2
Exchange current density	300 mA/cm^2
Limiting current density	900 mA/cm^2
GT cycle	
PR	5, 7, 10, 15
Polytropic efficiency	0.9
Mechanical efficiency (compression and expansion)	0.98
Final exhaust temperature	423 K
Minimum temperature approach (HR unit)	20 K
Pressure drop	
SOFC cell	3%
Combustor	2%
EC	2%
HF	2%
Heat exchanger (each)	2%
Bottoming ST cycle	
HPST inlet steam (pressure/temperature)	160 bar/813 K
IPST inlet steam (pressure/temperature)	35 bar/813 K
LPST inlet steam (pressure/temperature)	3.1 bar/623 K
Isentropic efficiency	0.9
Mechanical efficiency	0.97
Water feed pump efficiency	0.92

Systems were assessed in terms of thermal efficiency and specific work of the overall system. The fuel utilization (U_f) factor and working PR were varied with a constant air utilization (U_a) factor. It is noted that an increase in U_f factor means less amount of fuel being burnt in the CC, leading to a decrease in turbine inlet temperature (TIT). The U_f factor was kept in the range that gives resulting TIT between 1000 and 1700 K for a given PR. It was confirmed that there is sufficient oxygen remaining in the air stream after the SOFC module to react with fuel in the combustor as long as the U_f value is greater than the U_a value. Specific work (w) and thermal efficiency (η_{th}) (lower heating value based) of the overall system are described as

$$w = \frac{W_{GT} + W_{ST} + W_{FC} - W_{CP}}{m_{air}} \quad (1)$$

$$\eta_{th} = \frac{m_{air} w}{m_f \mathrm{LHV}_f} \quad (2)$$

where W_{GT}, W_{ST}, and W_{FC} denote work produced in the GT, ST, and fuel cell (SOFC), respectively. W_{CP} denotes

compressor work, while m_{air} and m_f denote the mass flow rate of the air stream and fuel stream, respectively. LHV_f denotes the specific lower heating value of fuel. For the SOFC–HAT system case, W_{CP} represents the summation of compressor work in the LCP and HCP.

3. Results and discussion

3.1. Effects of TIT and PR on system performance

3.1.1. SOFC–STIG system

Table 2 summarizes the simulation results of the SOFC–STIG system. It was observed that TIT increases with a decrease in U_f factor. Although a rise in TIT normally increases GT efficiency, overall thermal efficiency was observed to decrease with increasing TIT (decreasing U_f factor) for all PRs because SOFC efficiency exceeds that of GT. Water consumption for steam injection depends on the GT exhaust temperature because only the steam recuperation feature is employed to recover exhaust heat by means of steam injection. At higher TIT, the water consumption was observed to become larger for a given PR, as shown in Table 2. This means the specific mass flow through the GT increased, increasing net specific work. Fig. 4 shows the thermal efficiency, the specific work, and the water consumption plotted against TIT at different PRs. For a given TIT, the thermal efficiency improves as PR increases, while

Table 2
Simulation results of SOFC–STIG system

PR	5	5	5	5	5	5	5	5	
Fuel utilization, U_f (–)	0.80	0.75	0.70	0.65	0.60	0.55	0.50	0.45	
Air utilization, U_a (–)	0.30	0.30	0.30	0.30	0.30	0.30	0.30	0.30	
Compressed air temperature (K)	505	505	505	505	505	505	505	505	
TIT (K)	1025	1074	1129	1190	1257	1333	1419	1517	
Turbine outlet temperature (K)	746	786	830	880	935	998	1069	1152	
Final exhaust temperature (K)	423	423	423	423	423	423	423	423	
Water consumption (kg-water/kg-air)	0.138	0.156	0.178	0.202	0.230	0.263	0.302	0.349	
Steam temperature (K)	727	766	811	860	915	978	1049	1132	
Specific work (kJ/kg-air)	720	754	793	839	893	958	1037	1134	
Thermal efficiency (–)	0.5452	0.5354	0.5259	0.5166	0.5076	0.4990	0.4908	0.4832	
PR	7	7	7	7	7	7	7	7	7
Fuel utilization, U_f (–)	0.85	0.80	0.75	0.70	0.65	0.60	0.55	0.50	0.45
Air utilization, U_a (–)	0.30	0.30	0.30	0.30	0.30	0.30	0.30	0.30	0.30
Compressed air temperature (K)	560	560	560	560	560	560	560	560	560
TIT (K)	1018	1062	1110	1163	1222	1287	1360	1443	1538
Turbine outlet temperature (K)	688	721	758	798	844	895	953	1019	1096
Final exhaust temperature (K)	423	423	423	423	423	423	423	423	423
Water consumption (kg-water/kg-air)	0.111	0.127	0.144	0.163	0.185	0.211	0.241	0.277	0.321
Steam temperature (K)	668	701	738	779	824	875	933	999	1076
Specific work (kJ/kg-air)	713	747	786	830	881	941	1014	1101	1209
Thermal efficiency (–)	0.5742	0.5660	0.5579	0.5500	0.5423	0.5349	0.5278	0.5212	0.5152
PR	10	10	10	10	10	10	10	10	10
Fuel utilization, U_f (–)	0.85	0.80	0.75	0.70	0.65	0.60	0.55	0.50	0.45
Air utilization, U_a (–)	0.30	0.30	0.30	0.30	0.30	0.30	0.30	0.30	0.30
Compressed air temperature (K)	623	623	623	623	623	623	623	623	623
TIT (K)	1064	1107	1154	1205	1262	1326	1397	1478	1569
Turbine outlet temperature (K)	668	699	732	770	812	860	913	975	1046
Final exhaust temperature (K)	423	423	423	423	423	423	423	423	423
Water consumption (kg-water/kg-air)	0.103	0.117	0.133	0.151	0.171	0.195	0.223	0.256	0.296
Steam temperature (K)	648	679	713	750	792	840	893	955	1026
Specific work (kJ/kg-air)	733	770	812	860	917	983	1062	1157	1275
Thermal efficiency (–)	0.5898	0.5831	0.5766	0.5703	0.5642	0.5584	0.5528	0.5477	0.5431
PR	15	15	15	15	15	15	15		
Fuel utilization, U_f (–)	0.75	0.70	0.65	0.60	0.55	0.50	0.45		
Air utilization, U_a (–)	0.30	0.30	0.30	0.30	0.30	0.30	0.30		
Compressed air temperature (K)	703	703	703	703	703	703	703		
TIT (K)	1211	1261	1317	1378	1447	1526	1615		
Turbine outlet temperature (K)	709	744	783	826	876	933	998		
Final exhaust temperature (K)	423	423	423	423	423	423	423		
Water consumption (kg-water/kg-air)	0.123	0.139	0.158	0.180	0.205	0.235	0.272		
Steam temperature (K)	689	724	763	807	856	913	978		
Specific work (kJ/kg-air)	834	887	948	1020	1105	1208	1335		
Thermal efficiency (–)	0.5925	0.5879	0.5835	0.5793	0.5753	0.5718	0.5687		

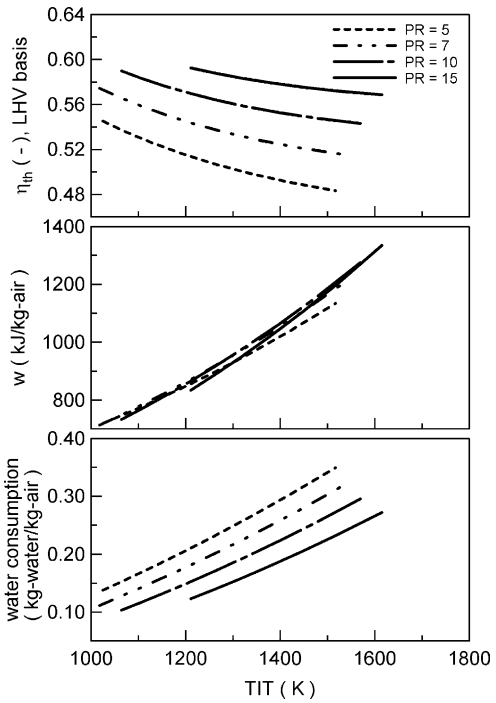

Fig. 4. Influences of TIT and PR on thermal efficiency, specific work and water consumption in a SOFC–STIG system.

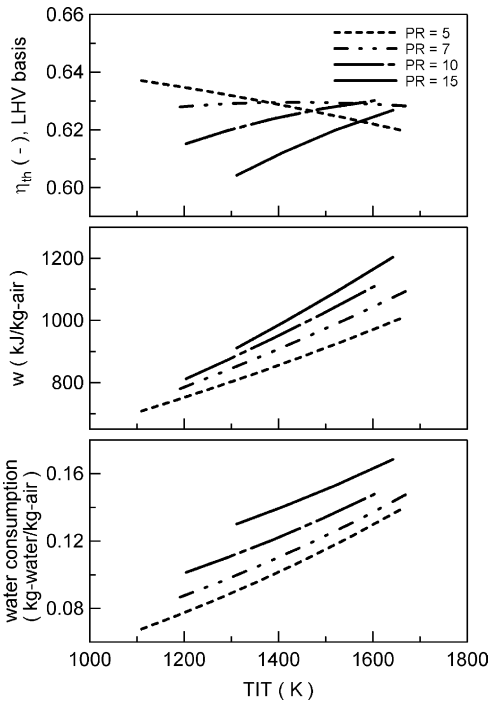

Fig. 5. Influences of TIT and PR on thermal efficiency, specific work and water consumption in a SOFC–STIG system with APH.

the specific work is not significantly changed with PRs. In general, an increase in PR reduces GT exhaust temperature at a constant TIT. This decreases the water consumption for the steam injection, as can be seen in Fig. 4. Consequently, the amount of heat required in the GT combustor to heat the steam is reduced at higher PR, indicating the increase in U_f factor. Therefore, the increase in PR leads to the improvement of overall thermal efficiency.

3.1.2. SOFC–STIG with APH system

Table 3 gives the simulation results for the SOFC–STIG with APH system. Fig. 5 depicts thermal efficiency, specific work, and water consumption as a function of TIT and PR. In this system, the GT exhaust is used to generate steam in the HRSG and to preheat the compressed air stream in the recuperator (APH). These configurations are similar to the SOFC–GT with heat and steam recuperation features [14]. In contrast to the simple SOFC–STIG system, upward trends of the thermal efficiency with increasing TIT were observed for all PRs except for PR = 5. This may be due to integration of both heat and steam recuperation features by means of APH and steam injection. These features are considered to overcome the adverse effect of increasing TIT with the reduction of U_f factor at high PRs. The water consumption in the HRSG and the specific work were observed to increase with TIT for all PRs.

In addition, Fig. 5 shows the influence of PR on system performance at a constant TIT. An increase in PR was found to increase both specific work and water consumption for the whole range of TIT. On the other hand, different dependency of PR on the thermal efficiency was observed. The thermal efficiency gradually decreases with increasing PR at low TITs, while the opposite trend was observed at high TITs. Since an increase in PR reduces GT outlet temperature, addition of fuel consumption to the GT combustor is required to maintain the same TIT. This means that the increase in PR reduces the U_f factor. Thus, a higher PR gives lower thermal efficiency at low TITs, as can be seen in Fig. 5. In contrast, an increase in thermal efficiency with increasing PR at high TITs was observed at high TITs. It was speculated that the GT efficiency improvement by increasing PR becomes more substantial at high TITs, overcoming the adverse effect of PR.

3.1.3. SOFC–GT/ST system

Table 4 summarizes the key simulation results of the SOFC–GT/ST system. Steam temperatures and pressures in the bottoming ST cycle were kept constant in this system despite a change of GT exhaust temperature with variations of U_f factor and PR. Hence, the minimum temperature approach in the HRSG was not constant at 20 K and became larger with an increase in the GT exhaust temperature. Thermal efficiency, specific work, and water consumption were plotted against TIT as a function of PR in Fig. 6. It was observed that an increase in TIT reduces the thermal efficiency. This is attributed to adverse effect of the decrease in U_f factor and the increase in the minimum temperature approach. The specific work and the water consumption were found to increase with increasing TIT. Effects of PR on thermal efficiency and water consumption are similar to those

Table 3
Simulation results of SOFC–STIG with APH system

PR	5	5	5	5	5	5	5
Fuel utilization, U_f (–)	0.95	0.90	0.85	0.80	0.75	0.70	0.65
Air utilization, U_a (–)	0.30	0.30	0.30	0.30	0.30	0.30	0.30
Compressed air temperature (K)	505	505	505	505	505	505	505
Preheated air temperature (K)	747	795	847	903	964	1030	1101
TIT (K)	1109	1186	1268	1356	1450	1551	1661
Turbine outlet temperature (K)	807	868	933	1003	1079	1161	1250
Final exhaust temperature (K)	423	423	423	423	423	423	423
Water consumption (kg-water/kg-air)	0.068	0.076	0.085	0.096	0.108	0.122	0.139
Steam temperature (K)	787	848	913	983	1059	1141	1230
Specific work (kJ/kg-air)	708	745	786	832	883	941	1007
Thermal efficiency (–)	0.6371	0.6351	0.6329	0.6302	0.6272	0.6238	0.6199
PR	7	7	7	7	7	7	
Fuel utilization, U_f (–)	0.85	0.80	0.75	0.70	0.65	0.60	
Air utilization, U_a (–)	0.30	0.30	0.30	0.30	0.30	0.30	
Compressed air temperature (K)	560	560	560	560	560	560	
Preheated air temperature (K)	762	813	869	929	994	1067	
TIT (K)	1191	1276	1366	1464	1571	1686	
Turbine outlet temperature (K)	813	877	946	1021	1103	1193	
Final exhaust temperature (K)	423	423	423	423	423	423	
Water consumption (kg-water/kg-air)	0.087	0.096	0.106	0.118	0.133	0.150	
Steam temperature (K)	793	857	926	1001	1083	1173	
Specific work (kJ/kg-air)	780	830	886	950	1022	1106	
Thermal efficiency (–)	0.6279	0.6290	0.6295	0.6296	0.6292	0.6282	
PR	10	10	10	10	10		
Fuel utilization, U_f (–)	0.80	0.75	0.70	0.65	0.60		
Air utilization, U_a (–)	0.30	0.30	0.30	0.30	0.30		
Compressed air temperature (K)	623	623	623	623	623		
Preheated air temperature (K)	737	787	841	902	968		
TIT (K)	1204	1292	1387	1490	1603		
Turbine outlet temperature (K)	765	827	896	971	1055		
Final exhaust temperature (K)	423	423	423	423	423		
Water consumption (kg-water/kg-air)	0.101	0.110	0.121	0.133	0.148		
Steam temperature (K)	745	807	876	951	1035		
Specific work (kJ/kg-air)	812	873	941	1019	1109		
Thermal efficiency (–)	0.6152	0.6197	0.6238	0.6273	0.6302		
PR	15	15	15	15			
Fuel utilization, U_f (–)	0.70	0.65	0.60	0.55			
Air utilization, U_a (–)	0.30	0.30	0.30	0.30			
Compressed air temperature (K)	703	703	703	703			
Preheated air temperature (K)	762	816	877	944			
TIT (K)	1312	1411	1521	1642			
Turbine outlet temperature (K)	776	844	920	1005			
Final exhaust temperature (K)	423	423	423	423			
Water consumption (kg-water/kg-air)	0.130	0.141	0.153	0.168			
Steam temperature (K)	758	824	900	985			
Specific work (kJ/kg-air)	912	995	1091	1204			
Thermal efficiency (–)	0.6043	0.6124	0.6200	0.6268			

in the case of the simple SOFC–STIG system (see Figs. 4 and 6).

3.1.4. SOFC–HAT system

Table 5 presents the key simulation results of the SOFC–HAT system. In addition to the U_f factor and PR, temperature of the depleted air stream prior to entering the HF varied as 353, 363, and 373 K. At the same PR and U_f factor, we found that the depleted air temperature of 353 K yields the highest efficiency in spite of the slight difference in TIT. This is caused by an increase of the heat recuperation rate in the HR unit. For the depleted air temperature of 353 K, influences of TIT and PR on thermal efficiency, specific work, and water consumption are shown in Fig. 7. The thermal efficiency was observed to rise up as TIT increases for a given PR. This is due to the significant improvement of GT efficiency with increasing TIT by enhancing energy recuperation from the GT exhaust. The improvement of GT efficiency overcomes the unfavorable effect of the increase in TIT (the decrease in U_f factor), increasing the overall thermal

Table 4
Simulation results of SOFC–GT/ST system

PR	5	5	5	5	5	5
Fuel utilization, U_f (–)	0.75	0.70	0.65	0.60	0.55	0.50
Air utilization, U_a (–)	0.30	0.30	0.30	0.30	0.30	0.30
Compressed air temperature (K)	502	502	502	502	502	502
TIT (K)	1154	1223	1300	1387	1487	1602
Turbine outlet temperature (K)	842	896	957	1026	1106	1198
Final exhaust temperature (K)	423	423	423	423	423	423
Water consumption (kg-water/kg-air)	0.123	0.140	0.161	0.185	0.214	0.248
Steam temperature (K)	813	813	813	813	813	813
Specific work (kJ/kg-air)	876	929	991	1062	1145	1245
Thermal efficiency (–)	0.6221	0.6161	0.6098	0.6032	0.5964	0.5892
PR	7	7	7	7	7	7
Fuel utilization, U_f (–)	0.75	0.70	0.65	0.60	0.55	0.50
Air utilization, U_a (–)	0.30	0.30	0.30	0.30	0.30	0.30
Compressed air temperature (K)	556	556	556	556	556	556
TIT (K)	1198	1267	1343	1431	1530	1645
Turbine outlet temperature (K)	815	866	924	989	1064	1152
Final exhaust temperature (K)	423	423	423	423	423	423
Water consumption (kg-water/kg-air)	0.114	0.131	0.150	0.173	0.200	0.232
Steam temperature (K)	813	813	813	813	813	813
Specific work (kJ/kg-air)	894	950	1014	1089	1177	1281
Thermal efficiency (–)	0.6346	0.6295	0.6242	0.6186	0.6127	0.6065
PR	10	10	10	10	10	
Fuel utilization, U_f (–)	0.70	0.65	0.60	0.55	0.50	
Air utilization, U_a (–)	0.30	0.30	0.30	0.30	0.30	
Compressed air temperature (K)	620	620	620	620	620	
TIT (K)	1318	1395	1482	1581	1695	
Turbine outlet temperature (K)	839	893	955	1026	1109	
Final exhaust temperature (K)	423	423	423	423	423	
Water consumption (kg-water/kg-air)	0.122	0.140	0.162	0.187	0.218	
Steam temperature (K)	813	813	813	813	813	
Specific work (kJ/kg-air)	967	1035	1113	1205	1314	
Thermal efficiency (–)	0.6411	0.6368	0.6323	0.6275	0.6222	
PR	15	15	15			
Fuel utilization, U_f (–)	0.65	0.60	0.55			
Air utilization, U_a (–)	0.30	0.30	0.30			
Compressed air temperature (K)	699	699	699			
TIT (K)	1461	1547	1646			
Turbine outlet temperature (K)	864	922	988			
Final exhaust temperature (K)	423	423	423			
Water consumption (kg-water/kg-air)	0.131	0.151	0.174			
Steam temperature (K)	813	813	813			
Specific work (kJ/kg-air)	1053	1135	1231			
Thermal efficiency (–)	0.6481	0.6448	0.6411			

efficiency. The elevation of TIT was observed to increase both specific work and water consumption in this system.

Effect of PR on system performance was found to be somewhat similar to that in the case of the SOFC–STIG with APH system because this system also incorporates heat and steam recuperation features, just as the SOFC–STIG with APH system does. An increase in PR reduces the thermal efficiency for a given TIT, while the specific work is increased corresponding to the increase in water consumption.

3.2. Comparison of the four systems' performance

Figs. 8–10 show the comparative results of thermal efficiency, specific work, and water consumption, respectively, for four systems. Fig. 11 depicts energy flow diagrams of four systems at the TIT of 1450 K and PR of 7. At a constant TIT, the SOFC–HAT system was observed to have the highest thermal efficiency, while the simple SOFC–STIG system yields the lowest thermal efficiency. Advantages of HAT cycle over other GT cycles have also been mentioned in the literature [3–8]. Improvement in efficiency of the HAT cycle is due to intercooling and energy recuperation features. The SOFC–HAT system engages both heat and steam recuperation, reducing the amount of water consumption (see Fig. 10). In addition, some amount of heat is extracted from the hot compressed air to heat water before feeding it to the HF. As a result, this system requires less heat supplied from fuel than other systems to achieve the same TIT level,

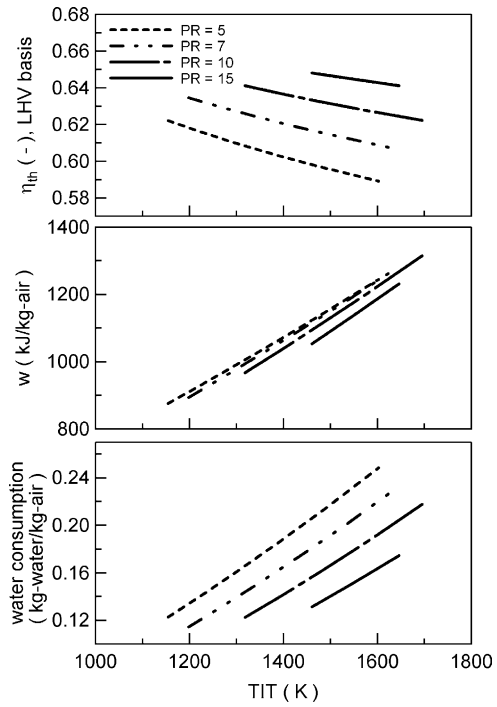

Fig. 6. Influences of TIT and PR on thermal efficiency, specific work and water consumption in a SOFC–GT/ST system.

as can be seen in Fig. 11. In general, a high U_f factor for SOFC–GT systems is preferable because the SOFC is more efficient than the GT. As shown in Fig. 11, the SOFC–HAT system was found to have a high U_f factor, engendering

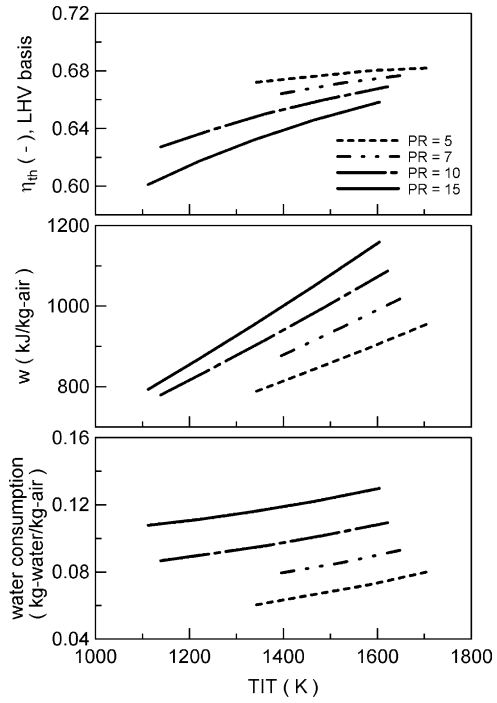

Fig. 7. Influences of TIT and PR on thermal efficiency, specific work and water consumption in a SOFC–HAT system (depleted air temperature of 353 K).

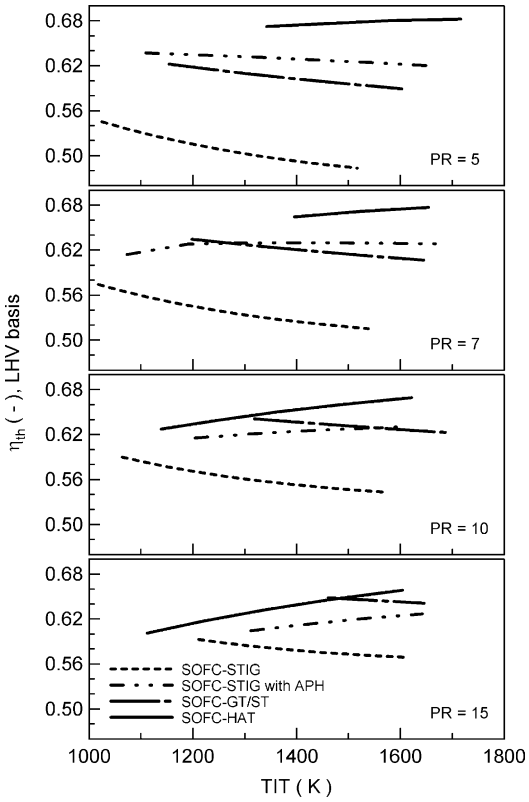

Fig. 8. Comparison results of thermal efficiency as a function of TIT for each PR.

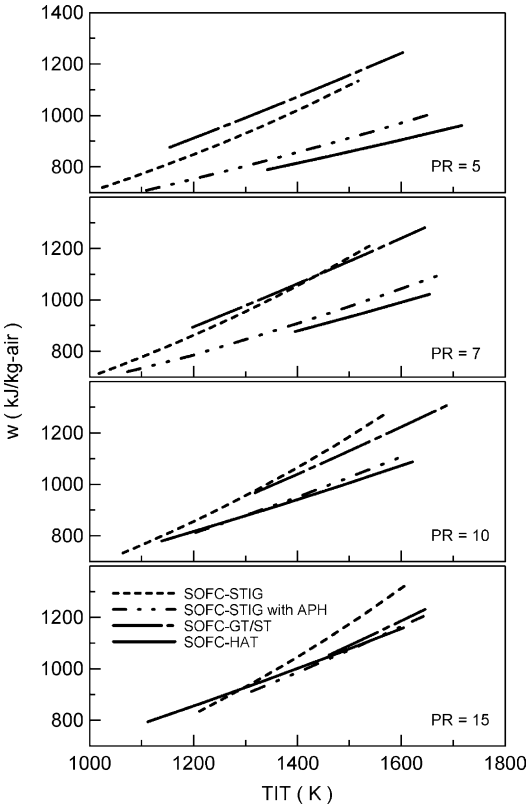

Fig. 9. Comparison results of specific work as a function of TIT for each PR.

Table 5
Simulation results of SOFC–HAT system

PR	5	5	5	5	5	5	5	5	5	5	5	5			
Fuel utilization, U_f (–)	0.90	0.90	0.90	0.85	0.85	0.85	0.80	0.80	0.80	0.75	0.75	0.75			
Air utilization, U_a (–)	0.30	0.30	0.30	0.30	0.30	0.30	0.30	0.30	0.30	0.30	0.30	0.30			
Depleted air temperature (K)	353	363	373	353	363	373	353	363	373	353	363	373			
TIT (K)	1343	1342	1339	1458	1457	1456	1585	1581	1580	1716	1712	1711			
Turbine outlet temperature (K)	993	992	990	1084	1083	1083	1186	1183	1182	1291	1288	1287			
Final exhaust temperature (K)	423	423	423	423	423	423	423	423	423	423	423	423			
Water consumption (kg-water/kg-air)	0.061	0.061	0.063	0.066	0.067	0.068	0.072	0.074	0.075	0.081	0.082	0.083			
Humid temperature (K)	972	972	969	1063	1063	1063	1166	1162	1162	1271	1267	1267			
Specific work (kJ/kg-air)	789	786	783	840	837	835	898	894	892	961	957	954			
Thermal efficiency (–)	0.6722	0.6699	0.6669	0.6761	0.6739	0.6718	0.6802	0.6775	0.6755	0.6822	0.6797	0.6778			
PR	7	7	7	7	7	7	7	7	7						
Fuel utilization, U_f (–)	0.80	0.80	0.80	0.75	0.75	0.75	0.70	0.70	0.70						
Air utilization, U_a (–)	0.30	0.30	0.30	0.30	0.30	0.30	0.30	0.30	0.30						
Depleted air temperature (K)	353	363	373	353	363	373	363	373	373						
TIT (K)	1396	1396	1394	1522	1519	1517	1651	1649	1646						
Turbine outlet temperature (K)	968	968	967	1064	1062	1060	1163	1161	1159						
Final exhaust temperature (K)	423	423	423	423	423	423	423	423	423						
Water consumption (kg-water/kg-air)	0.079	0.080	0.082	0.085	0.087	0.088	0.095	0.096	0.096						
Humid temperature (K)	947	948	947	1044	1042	1041	1143	1141	1139						
Specific work (kJ/kg-air)	877	874	871	946	942	938	1018	1014	1013						
Thermal efficiency (–)	0.6642	0.6621	0.6594	0.6715	0.6689	0.6664	0.6746	0.6722	0.6717						
PR	10	10	10	10	10	10	10	10	10	10	10	10	10	10	10
Fuel utilization, U_f (–)	0.85	0.85	0.85	0.80	0.80	0.80	0.75	0.75	0.75	0.70	0.70	0.70	0.65	0.65	0.65
Air utilization, U_a (–)	0.30	0.30	0.30	0.30	0.30	0.30	0.30	0.30	0.30	0.30	0.30	0.30	0.30	0.30	0.30
Depleted air temperature (K)	353	363	373	353	363	373	353	363	373	353	363	373	353	363	373
TIT (K)	1139	1137	1134	1245	1244	1239	1361	1358	1357	1485	1484	1481	1622	1618	1617
Turbine outlet temperature (K)	721	719	718	795	795	792	878	876	875	967	966	964	1066	1064	1063
Final exhaust temperature (K)	423	423	423	423	423	423	423	423	423	423	423	423	423	423	423
Water consumption (kg-water/kg-air)	0.087	0.088	0.090	0.091	0.092	0.094	0.095	0.097	0.098	0.102	0.103	0.105	0.109	0.111	0.112
Humid temperature (K)	701	699	698	775	775	771	858	856	856	947	946	944	1046	1044	1043
Specific work (kJ/kg-air)	779	775	770	843	840	834	915	911	907	996	992	987	1087	1083	1079
Thermal efficiency (–)	0.6272	0.6237	0.6201	0.6387	0.6360	0.6320	0.6501	0.6469	0.6444	0.6598	0.6575	0.6545	0.6691	0.6664	0.6641
PR	15	15	15	15	15	15	15	15	15	15	15	15	15	15	15
Fuel utilization, U_f (–)	0.80	0.80	0.80	0.75	0.75	0.75	0.70	0.70	0.70	0.65	0.65	0.65	0.60	0.60	0.60
Air utilization, U_a (–)	0.30	0.30	0.30	0.30	0.30	0.30	0.30	0.30	0.30	0.30	0.30	0.30	0.30	0.30	0.30
Depleted air temperature (K)	353	363	373	353	363	373	353	363	373	353	363	373	353	363	373
TIT (K)	1112	1109	1108	1220	1217	1216	1337	1335	1331	1465	1462	1459	1604	1601	1599
Turbine outlet temperature (K)	646	644	643	717	715	714	795	794	791	881	880	877	977	975	974
Final exhaust temperature (K)	423	423	423	423	423	423	423	423	423	423	423	423	423	423	423
Water consumption (kg-water/kg-air)	0.108	0.110	0.111	0.111	0.113	0.115	0.116	0.118	0.119	0.122	0.124	0.125	0.130	0.131	0.133
Humid temperature (K)	626	624	624	697	695	694	775	774	771	861	860	857	956	955	953
Specific work (kJ/kg-air)	794	788	784	869	864	859	954	949	944	1049	1045	1040	1159	1154	1150
Thermal efficiency (–)	0.6011	0.5971	0.5937	0.6173	0.6135	0.6103	0.6320	0.6290	0.6255	0.6459	0.6431	0.6399	0.6584	0.6558	0.6533

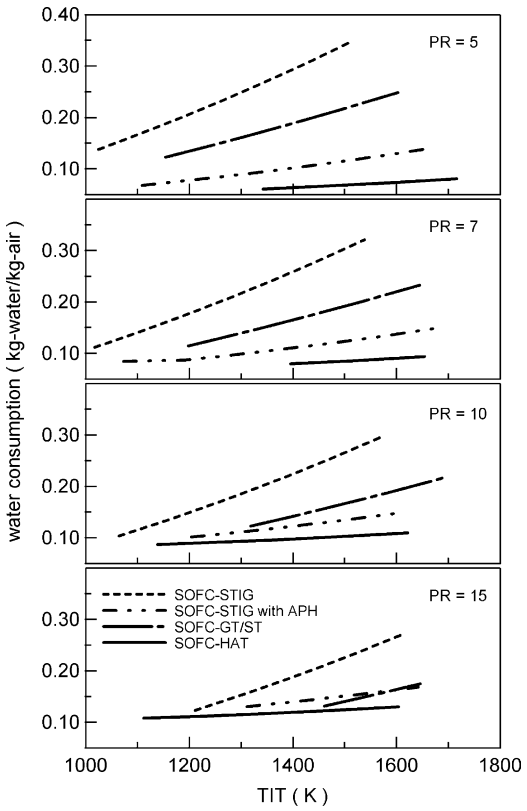

Fig. 10. Comparison results of water consumption as a function of TIT for each PR.

high thermal efficiency. On the other hand, the SOFC–STIG system requires great water consumption because of employing only steam recuperation. Hence, this system needs additional heat (fuel) to heat the injected steam to operating TIT in the GT combustor. This reduces the thermal efficiency of the system.

Fig. 8 shows that the thermal efficiency of the SOFC–STIG with APH system is higher than that of the SOFC–GT/ST system for a given TIT. However, a reverse trend was observed at a relatively high PR. This is due to the opposite effect of increasing PR on the thermal efficiency between the SOFC–STIG with APH system and the SOFC–GT/ST system (see Figs. 5 and 6). Similar to the SOFC–HAT system, the SOFC–STIG with APH system employs both heat and steam recuperation, leading to low water consumption. Thus, the high thermal efficiency is the result of the high U_f factor, as can be seen in Fig. 11. In the SOFC–GT/ST system, steam is not recuperated, but is individually utilised and expanded in a ST cycle. Steam can be expanded into a very low-pressure level (condensing pressure) in the ST cycle. This has been proved to be more powerful than simultaneous expansion with the combustion gas like in the STIG cycle [3]. As a result, the SOFC–GT/ST system is more efficient than the SOFC–STIG system. Furthermore, the steam in the ST cycle can be recirculated, mitigating the problem of additional water treatment. However, the

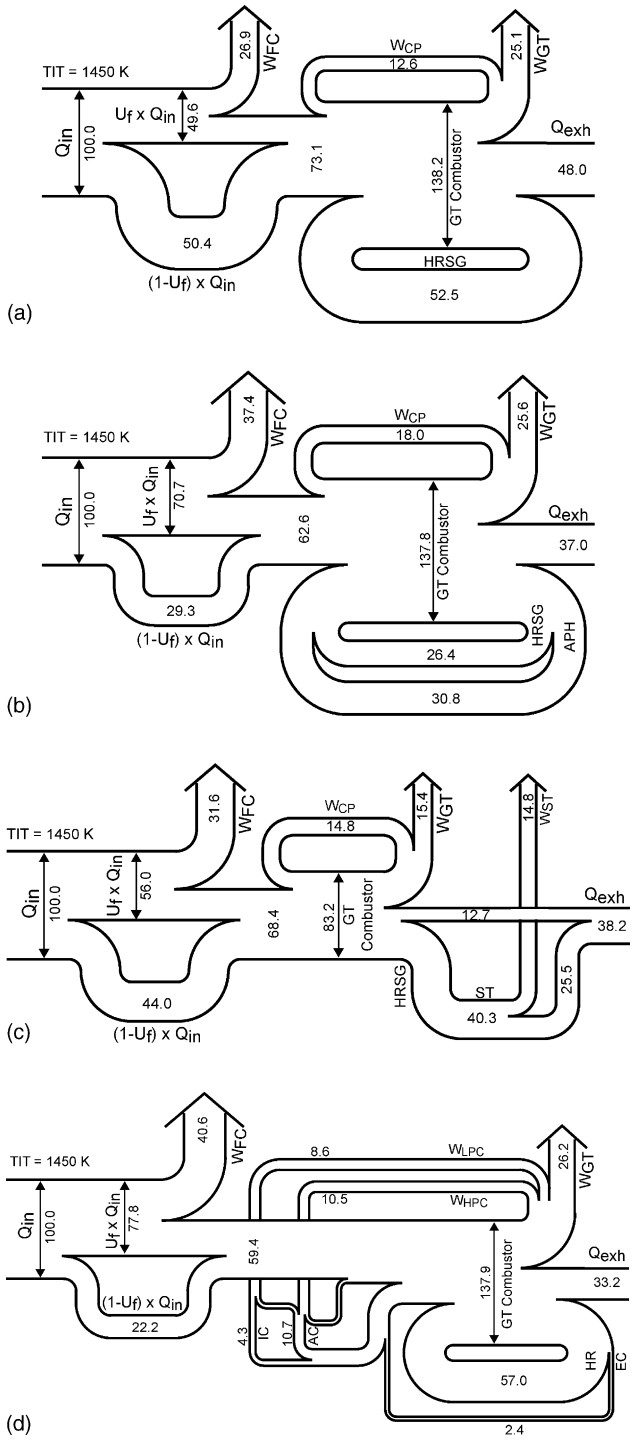

Fig. 11. Energy flow diagrams of four systems for TIT = 1450 K and PR = 7: (a) SOFC–STIG; (b) SOFC–STIG with APH; (c) SOFC–GT/ST; (d) SOFC–HAT.

requirement of the ST cycle in addition to the GT cycle renders this system complex and costly in comparison with other systems.

Fig. 9 shows that the SOFC–HAT system exhibits the lowest specific work especially at low PRs in spite of high thermal efficiency. This is attributable to low water

consumption in the SOFC–HAT system, as shown in Fig. 10. At relatively high PRs, the specific work of the SOFC–HAT system seems to be competitive with other systems. Therefore, the SOFC–HAT system has the best performance in terms of thermal efficiency and specific work output when operates at high TIT and PR. The SOFC–STIG with APH system and the SOFC–HAT system were found to require low water consumption, corresponding to low specific work of both systems (Fig. 9). This is because both systems engage not only steam recuperation, but also heat recuperation in HR of the GT exhaust. Even at high TITs, low water consumption is another benefit of the SOFC–HAT system in terms of water treatment.

4. Conclusions

Combinations of SOFC and several advanced GT cycles were studied and evaluated. It was found that system operation at high TIT does not boost overall thermal efficiency in the SOFC–STIG and the SOFC–GT/ST systems. The positive effect of increasing TIT on the thermal efficiency was observed in the SOFC–HAT system and the SOFC–STIG with APH system, especially at a high PR. Specific work increases with elevation of TIT for all systems, corresponding to water consumption results. For a given TIT, effect of PR on system performance in the SOFC–STIG system is similar to those in the SOFC–GT/ST system. The increase in PR raises the thermal efficiency and reduces the water consumption. The effect of PR found to be opposite in the SOFC–STIG with APH system to that in the SOFC–HAT system. The thermal efficiency decreases with increasing PR, while the specific work and the water consumption increase. Regarding comparison results for the four systems, the combination of SOFC and HAT cycle yields the highest overall efficiency. The SOFC–STIG system and the SOFC–GT/ST system show similar specific work higher than the other two systems at the same PR. However, the SOFC–STIG system was found to consume more supplied water compared to the SOFC–GT/ST system. The SOFC–HAT system gives the lowest specific work at low PRs, corresponding to the lowest water consumption. It is noteworthy that the SOFC–HAT system is a promising system with high efficiency and specific work output when the system operates at high TIT and PR condition. Furthermore, the system requires less water consumption, reducing the problem of water supply.

Acknowledgements

The authors acknowledge financial support from the Core Research for Evolutional Science and Technology (CREST) and the New Energy and Industrial Development Organization (NEDO) of Japan, and collaboration from the Cooperative Research Centre for Clean Power from Lignite, Australia.

References

[1] K.F. Kesser, M.A. Hoffman, J.W. Baughn, Trans. ASME J. Eng. Gas Turbines Power 116 (1994) 277–284.
[2] M. De Paepe, E. Dick, Int. J. Energy Res. 24 (2000) 1081–1107.
[3] T.S. Kim, C.H. Song, S.T. Ro, S.K. Kauh, Energy 25 (2000) 313–324.
[4] W.L.R. Gallo, Energy Conserv. Manage. 38 (1997) 1595–1604.
[5] A.D. Rao, US Patent 4 829 763 (1989).
[6] Y. Xiao, R. Cai, R. Lin, Energy Conserv. Manage. 38 (1997) 1605–1612.
[7] W.L.R. Gallo, G. Bidini, N. Bettagli, B. Facchini, Energy 22 (1997) 375–380.
[8] S.S. Stecco, U. Desideri, B. Facchini, N. Bettagli, ASME Paper 93-GT-77, 1993.
[9] J. Palsson, A. Selimovic, L. Sjunnesson, J. Power Sources 86 (2000) 442–448.
[10] A. Khandkar, J. Hartvigsen, S. Elangovan, Solid State Ionics 135 (2000) 325–330.
[11] K. Tanaka, C. Wen, K. Yamada, Fuel 79 (2000) 1493–1507.
[12] E. Riensche, E. Achenbach, D. Froning, M.R. Haines, W.K. Heidug, A. Lokurlu, S. von Andrian, J. Power Sources 86 (2000) 404–410.
[13] P. Costamagna, L. Magistri, A.F. Massardo, J. Power Sources 96 (2001) 352–368.
[14] P. Kuchonthara, S. Bhattacharya, A. Tsutsumi, J. Power Sources 117 (2003) 7–13.
[15] G. Lozza, P. Chiesa, L. DeVita, ASME J. Eng. Gas Turbines Power 118 (1996) 737–748.